

Detector-Device-Independent Quantum Key Distribution

Charles Ci Wen Lim,^{*} Boris Korzh,[†] Anthony Martin, Félix Bussi eres, Rob Thew, and Hugo Zbinden
Group of Applied Physics, University of Geneva, Switzerland.

Recently, a quantum key distribution (QKD) scheme based on entanglement swapping, called measurement-device-independent QKD (mdiQKD), was proposed to bypass all detector side-channel attacks. While mdiQKD is conceptually elegant and offers a supreme level of security, the experimental complexity is challenging for practical systems. For instance, it requires interference between two widely separated independent single-photon sources, and the rates are dependent on detecting two photons - one from each source. We present a QKD scheme that removes the need for a two-photon system and instead uses the idea of a two-qubit single-photon (TQSP) to significantly simplify the implementation and improve the efficiency of mdiQKD in several aspects.

I. INTRODUCTION

Quantum key distribution (QKD) enables the exchange of cryptographic keys between two spatially separated users, Alice and Bob, who are connected by a potentially insecure quantum channel [1, 2]. Importantly, unlike conventional key distribution schemes, the security of QKD depends only on the principles of quantum physics and can be proven information-theoretically secure. However, despite the potential of QKD, one still has to be prudent about potential side-channel attacks that may lead to security failures. For example, it has been shown that with detector blinding techniques, it is possible to remotely hack the measurement unit of some QKD systems [3]. Consequently, this allows the adversary to control the measurement unit and thus learn everything about the secret key. Although it is possible to implement appropriate countermeasures for specific attacks, one may be wary that the adversary could devise new detector control strategies, unforeseen by the legitimate parties.

To deal with all known and yet-to-be-discovered detector side-channel attacks, a measurement-device-independent QKD (mdiQKD) protocol was proposed [4]. It makes use of entanglement swapping [5–7] such that the measurement unit does not have to be trusted. In the scheme, Alice and Bob each randomly prepare one of the four Bennett Brassard (BB84) states [1] and send it to a third party, Charlie, who performs a Bell state measurement (BSM) on them. Then, Charlie announces the outcome of his measurement so that either Alice or Bob can flip her/his bit values to obtain a correlated bit string. Therefore, conceptually speaking, Charlie’s role is to introduce entanglement between Alice and Bob via an entangling measurement. Seen in this light, it is clear that Alice and Bob do not have to trust Charlie since any other non-entangling measurement would necessarily introduce some noise between them. Therefore, mdiQKD offers security against all possible detector side-channel attacks.

In practice, mdiQKD is implemented using phase-randomized weak coherent states (WCSs), where Alice and Bob send BB84 states using either time-bin encoded qubits [8, 9] or polarization-encoded qubits [10, 11]. Charlie’s measurement unit is realized with a linear-optical Bell-state analyzer (BSA). To meet the qubit assumption, as required by mdiQKD, Alice and Bob each randomly vary the intensity of their laser pulses and use the decoy-state method [12–14] to estimate the fraction of single-photon states sent and detected by Charlie. For the measurement unit, the states sent by Alice and Bob are mixed at a 50/50 beam-splitter (BS) and for the time-bin coding the output states are detected by two single-photon detectors (SPD), whilst for the polarization coding each output contains a polarizing BS (PBS) with a total of four SPDs for the outputs. By noting the pairwise detection pattern of the detectors, it is possible to identify which of the four Bell states has been projected.

One drawback of mdiQKD is the fact that it is rather inefficient in terms of secret bits per pulse sent by both parties. Firstly, it requires two-photon interference and its BSA using only linear optics is at most 50% efficient [15, 16]. The situation becomes worse, however, if one decides to use time-bin qubits, since one of the Bell states, Ψ^- , is projected by detecting two photons in the same detector but different temporal modes, which requires an SPD with a fast recovery time [17]. This ultimately limits the clock-rate of the system or forces the user to use just one Bell-state for the secret key generation. Secondly, when WCSs are used, the results from one of the bases cannot be used for the raw-key generation, since this has an inherent 25% error rate due to the Poissonian nature of the sources [8, 10]. Therefore, in the worst case scenario, only 12.5% of successful Bell state projections can be used for key generation, conditioned on compatible basis choices.

Further, a two-photon BSM relies on coincidence detections, meaning that the secret key rates (SKR) scale as $(\eta_{det}P_1(\mu))^2$, where η_{det} is the SPD detection efficiency and $P_1(\mu)$ is the probability of the source emitting a single-photon. Considering that the majority of QKD systems use WCSs, where $P_1(\mu) = \mu e^{-\mu}$ ($\mu < 1$ is the average photon number per pulse) and that typical SPD efficiencies are around 10% to 30%, this means

^{*} ciwen.lim@unige.ch
[†] boris.korzh@unige.ch

that the performance of the protocol would be considerably worse compared to prepare-and-measure (P&M) schemes using only a single source of WCSs. For an idea of the performance at long distances, one can refer to a recent mdiQKD implementation demonstrated over 200 km, which achieved a SKR of 0.009 bps [18]. Consider also a recent P&M implementation with a similar security parameter [19] and overall stability [20]. Comparing the secret key rate at the same loss (39.6 dB) and factoring out the higher clock rate, one still arrives at a SKR rate of around 10 bps, despite using more compact SPDs with lower detection efficiency. In addition, the technological overhead for mdiQKD is significantly larger due to the use of two-photon interference, requiring both photons to be indistinguishable in all degrees of freedom (DoFs): temporal, polarization and frequency. The resource overhead in the finite-key scenario [21] is also larger compared to common P&M schemes [20, 22], due to need to apply the decoy-state method twice (for each source), increasing the statistical fluctuations. For example, at 150 km, Alice and Bob would have to send at least 10^{14} laser pulses to Charlie before key distillation is possible [21].

In order to bridge the gap between the practicality of P&M schemes and additional security offered by mdiQKD, we propose a novel QKD scheme that overcomes the aforementioned limitations of mdiQKD but is still secure against all detector side-channel attacks. Our scheme, henceforth referred to as detector-device-independent QKD (ddiQKD), essentially follows the one of mdiQKD, however, instead of encoding separate qubits into two independent photons, we exploit the concept of a two-qubit single-photon (TQSP).

From a conceptual point of view, our scheme recognizes the fact that a single-photon state is a quantum information carrier and can be used to carry multiple independent qubits. The central idea is to first encode Alice’s BB84 qubit into a single-photon and then send it through a quantum channel to Bob, who encodes his BB84 qubit (using another DoF) into it. Then, following along the lines of mdiQKD, Bob sends the state to a BSM that entangles the two independent qubits. Importantly, this new paradigm shift towards using TQSP in the context of mdiQKD resolves most of the technical challenges faced by mdiQKD experiments. More specifically, our scheme has the following advantages (1) it requires only single-photon interference, (2) the linear-optical BSA is 100% efficient [23], (3) the secret key rate would scale linearly with the SPD detection efficiency since only single-photon detections are needed and (4) it is expected that in the finite-key scenario the minimum classical post-processing size would be similar to that of P&M QKD schemes.

While the concept of ddiQKD is fundamentally the same as mdiQKD, there are still some subtleties that need to be pointed out. For instance, in mdiQKD, the adversary can interact with Alice’s and Bob’s qubits, but in our scheme, the adversary can only interact with Al-

ice’s qubit. Furthermore, we extend the trusted device boundary in Bob’s laboratory to include the linear optical elements of the BSM, leaving only the single-photon detectors as untrusted devices. By untrusted devices, we mean that the adversary can have full control over their functionalities, e.g., she can control the response functions of the detectors [24]. Nevertheless, these untrusted detectors are located within Bob’s controlled laboratory and Bob only reveals if the BSM is successful or not (please refer to Sec. III for further discussion).

Therefore, as far as detector-side-channel attacks are concerned, our scheme is a more practical alternative to mdiQKD. To illustrate this point, we also provide a proof-of-principle experiment based on polarized heralded single-photons.

II. A DETECTOR-DEVICE-INDEPENDENT QKD SCHEME

The protocol closely follows mdiQKD. The key difference is that, instead of using two independent single-photon sources, the scheme uses the concept of a two-qubit single-photon (TQSP) to realize a complete and deterministic BSM. Here, we will make use of the polarization and spatial DoFs to encode the qubits of Alice and Bob, respectively. The protocol works as follows; see Fig. 1. Alice first prepares a qubit in the polarization DoF of a single-photon. This can be achieved using a heralded single-photon from spontaneous parametric downconversion (SPDC), or with a source of WCSs combined with the decoy-state method. Alice’s state $|\psi_A\rangle_p$ is chosen at random from the following set of “BB84” states:

$$|\psi_A\rangle_p \in_r \begin{cases} |+\rangle = \frac{1}{\sqrt{2}}(|H\rangle + |V\rangle), \\ |-\rangle = \frac{1}{\sqrt{2}}(|H\rangle - |V\rangle), \\ |+i\rangle = \frac{1}{\sqrt{2}}(|H\rangle + i|V\rangle), \\ |-i\rangle = \frac{1}{\sqrt{2}}(|H\rangle - i|V\rangle), \end{cases}$$

where the subscript p indicates this is a qubit in the polarization DoF of the photon. Alice sends $|\psi_A\rangle_p$ to Bob via an untrusted optical channel. Upon reception of the photon, Bob encodes his random qubit state $|\psi_B\rangle_s$ in another DoF of the photon. Here we use the spatial DoF (hence the subscript “ s ”). To achieve this, Bob sends the photon on a 50/50 BS; we denote $|u\rangle$ and $|\ell\rangle$ the states of the basis defined by the “upper” and “lower” arms after the BS, respectively. He then applies a phase φ chosen at random in the set $\{0, \pi/2, \pi, 3\pi/2\}$ on the lower arm to prepare the state $|\psi_B\rangle_s = (|u\rangle + e^{i\varphi}|\ell\rangle)$, yielding BB84 states on the spatial modes. Both DoFs have so far been created and manipulated independently of each other, and thus the two-qubit state can be written as $|\psi_A\rangle_p \otimes |\psi_B\rangle_s$.

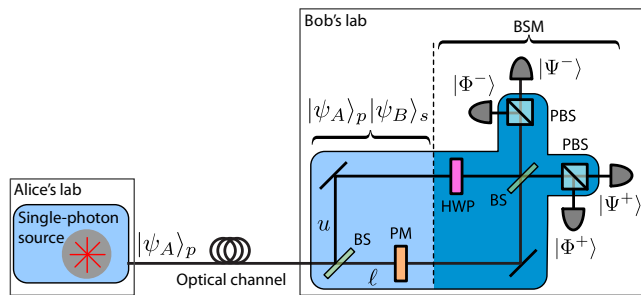


FIG. 1. The scheme exploits the concept of a single-photon two-qubit, where a single photon is used to encode both Alice's and Bob's qubits. Specifically, Alice encodes her qubit $|\psi_A\rangle_p$ in the polarization DoF of a single photon, sends it to Bob who encodes his qubit $|\psi_B\rangle_s$ in the spatial DoF using a 50/50 beam splitter (BS) and a phase modulator (PM). Bob then performs a complete and deterministic Bell-State measurement (BSM) on both qubits using a half-wave plate (HWP), polarizing beam splitters (PBS) and single-photon detectors (SPDs).

Let us now define the following Bell states:

$$|\Phi^\pm\rangle = \frac{1}{\sqrt{2}}(|H\rangle_p|u\rangle_s \pm |V\rangle_p|\ell\rangle_s), \quad (1)$$

$$|\Psi^\pm\rangle = \frac{1}{\sqrt{2}}(|H\rangle_p|\ell\rangle_s \pm |V\rangle_p|u\rangle_s). \quad (2)$$

A complete and deterministic BSM of these states is realized by first applying the unitary transformation $|Hu\rangle \rightarrow |Vu\rangle$ and $|Vu\rangle \rightarrow |Hu\rangle$ on the upper arm using a half-wave plate (HWP), followed by recombination of the arms on a 50/50 beam splitter, and finally by a projection in the $\{|H\rangle, |V\rangle\}$ basis using two PBSs on the two output arms followed by four SPDs. In this way, a click on each SPD corresponds to a projection on one of the four Bell states; see Fig. 1.

To show how the raw key establishment functions, let us first define the mutually unbiased bases $\mathcal{B}_X = \{|+\rangle, |-\rangle\}$ and $\mathcal{B}_Y = \{|+i\rangle, |-i\rangle\}$. The bit to be established is encoded in Alice's state, i.e. $|+\rangle$ and $|+i\rangle$ encode bit 0, and $|-\rangle$ and $|-i\rangle$ encode bit 1. After the measurement phase, Bob uses a public and authenticated channel to announce the success of the BSM and reveals the basis he used to encode his qubit. Subsequently, Alice announces whether Bob's basis choice was compatible with hers. Bob can then determine Alice's bit value according to Table I. For example, if $|\psi_B\rangle_s = |+\rangle$, the bit is 0 if he detected $|\Phi^+\rangle$ or $|\Psi^+\rangle$, and 1 otherwise. Table I shows all possible cases. If more than one detector clicked, Bob announces a successful BSM and assigns a random bit value. Importantly, the knowledge of the bases used by Alice and Bob, along with which of the Bell states Bob obtained, does not reveal Alice's bit. Hence, the eavesdropper does not gain information on the key by controlling Bob's detectors.

a)		$ \Phi^+\rangle$				b)		$ \Psi^+\rangle$			
		+	-	+i	-i	+	-	+i	-i		
+	+	0.49	0.01	0.25	0.26	+	0.49	0.02	0.25	0.27	
-	+	0.01	0.50	0.25	0.27	-	0.00	0.50	0.27	0.24	
+i	+	0.27	0.26	0.01	0.48	+i	0.29	0.23	0.49	0.00	
-i	+	0.24	0.23	0.50	0.01	-i	0.23	0.25	0.01	0.55	
c)		$ \Psi^-\rangle$				d)		$ \Phi^-\rangle$			
		+	-	+i	-i	+	-	+i	-i		
+	+	0.00	0.48	0.28	0.25	+	0.00	0.47	0.25	0.25	
-	+	0.54	0.00	0.25	0.23	-	0.54	0.00	0.23	0.25	
+i	+	0.25	0.26	0.01	0.52	+i	0.26	0.26	0.48	0.00	
-i	+	0.26	0.24	0.50	0.01	-i	0.26	0.21	0.00	0.56	

TABLE I. Tables showing the expected and observed probabilities for each of the observed Bell state. For each table, rows and columns correspond to Alice's and Bob's states $|\psi_A\rangle_p$ and $|\psi_B\rangle_s$, respectively. For each $|\psi_A\rangle_p$ there are four possible $|\psi_B\rangle_s$; dark grey cells should happen with probability 1/2, white cells with probability 0 and light grey cells with probability 1/4. The experimentally observed probabilities are shown in each cell.

III. SECURITY DISCUSSION

In this section, we first discuss the security of the scheme in the context of multi-photon states and then provide a sketch of the security analysis (we defer the detailed analysis to a future paper).

To start with, we recall that Bob prepares his BB84 states by randomly adjusting the relative phase between the upper and lower arms of the interferometer (see Fig. 1). That is, the two-mode output light state after the phase modulator is described by $|\psi_B\rangle_s = (|u\rangle + e^{i\varphi}|\ell\rangle)$, where φ is randomly chosen from $\{0, \pi/2, \pi, 3\pi/2\}$. Strictly speaking, this mathematical description holds only if the light state entering the first beam-splitter is a single-photon excitation of a single optical-temporal mode. However, it is not possible to guarantee this. Indeed, since the input light state comes from the quantum channel, it is plausible that the adversary sends multi-photon states to break the qubit description for Bob's prepared states. Such an attack strategy may lead to bad security implications if the adversary can interact with Bob's prepared states, for instance, by making unambiguous state discrimination measurements on them [25]. Fortunately, as we mentioned earlier, this is not possible since the adversary can only interact with Alice's qubits and not with Bob's prepared states. Additionally, if the input light state is a multi-photon state, then, with very high probability, more than one detector will click, in which case Bob would pick a random bit value, increasing the errors in the raw bit string. This is due to the fact that the optical linear circuit of the BSM randomizes the encoded state. Moreover, it is intuitive that the adversary cannot gain more information by sending in multi-photon states since Bob only announces if the BSM is successful or not.

The security of our scheme crucially requires that the

final light state (the four-mode light state just before the single-photon detectors), i.e., taken over all possible encoding choices, is independent of the input light state. In particular, for any input state with a given n -photon excitation, the average final state after passing through the linear optical circuit is a fixed state. This requirement is in fact similar to the one used in the security analysis of BB84, where the average of the BB84 states has to be independent of the basis choice; otherwise, there would be basis-dependent flaws [26]. Once this requirement is met, the security of the scheme can be obtained following proof techniques for the BB84 QKD scheme.

A common method to prove the security of P&M QKD-schemes is to consider an equivalent entanglement-based version, where Alice and Bob make random measurements on bipartite quantum states distributed by the adversary. To this end, we point to a formalism that allows us to see Bob's linear optical circuit as random measurements made on some entangled bipartite state.

First, let us relate the two different DoFs, i.e. A_p , B_p denoting the polarization states of Alice and Bob respectively, while B_s denotes Bob's spatial state. Since Alice is able to prepare the four polarization BB84 states correctly, it is equivalent to consider the entanglement based version, where Alice first prepares a two-qubit maximally entangled state, $|\Phi^+\rangle$, and then performs a projective measurement on one half of the state to prepare the other half for Bob. Mathematically, we have, $M_x \otimes \mathbb{I}|\Phi^+\rangle\langle\Phi^+|_{A_p B_p} \otimes |s\rangle\langle s|_{B_s}$, where M_x is the positive-operator valued measure (POVM) element corresponding to preparation $x \in \{+, -, +i, -i\}$ and $|s\rangle_{B_s}$ is an auxiliary state related to the spatial DoF.

Second, Alice sends the quantum systems B_p and B_s using a single-photon through the quantum channel to Bob. At this point, the resulting state is not necessarily a single-photon state, e.g. it may be a multi-photon state. In this case, the state, after tracing out system A_p , is described by a bipartite density operator, $\rho_{C_p C_s}$, whose dimension is unknown but fixed, i.e., it could be any n -photon light state. Note that we changed the subscript B to C to reflect the action of the quantum channel. To proceed, we use a result from Ref. [27, Lemma. 1], which says that, if for any input state, the linear optical circuit (parameterized by φ) outputs a state that is fixed on the average, then the encoding can be seen as a purified measurement acting on the same input state and one half of a bipartite pure state, where the other half of the bipartite is the same output state. More formally, let the linear optical circuit be described by a set of completely positive trace-preserving maps, $\{\mathcal{E}_\varphi\}_\varphi$, taking the input quantum system C_s to an output quantum system D_s , such that for any input quantum state ρ_{C_s} , the output quantum state is fixed over all possible encoding choices, i.e., $1/4 \sum_\varphi \mathcal{E}_\varphi(\rho_{C_s}) = \rho_{D_s}$ for any ρ_{C_s} . Then, the linear optical circuit is equivalent to making a joint measurement $\{F_{C_s K_s}^\varphi\}_\varphi$ on the same input state, ρ_{C_s} , and one half of a bipartite pure state, $|\sigma\rangle_{K_s D_s}$, living in a joint quantum system $K_s \otimes D_s$, where the other half gives the

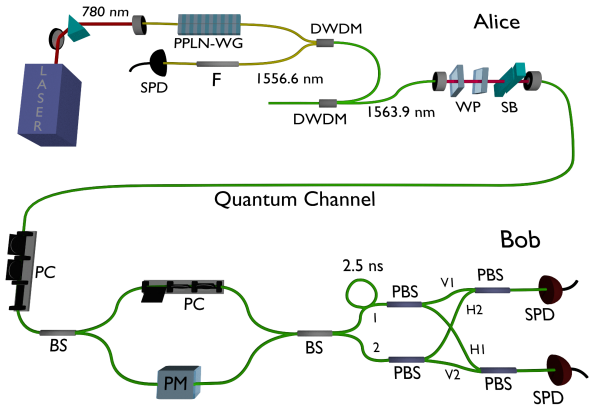


FIG. 2. Experimental realization of the ddiQKD protocol, based on a heralded single-photon source at a telecom wavelength, using mostly fiber based components. Labelled components include, dense wavelength division multiplexer (DWDM), bandpass filter (F), waveplates (WP), Soleil-Babinet compensator (SB), polarization controller (PC), phase modulator (PM), 50/50 beam splitter (BS), polarizing beam splitter (PBS) and single-photon detectors (SPD).

fixed state ρ_{D_s} . Therefore, from the security point of view, the purification provides a method to analyze the security of our scheme in an entanglement-based picture, in which Alice, Bob and the adversary share a tripartite entangled state. Note that the purification is valid only if the average output state of the linear optical circuit is independent of the input state. This assumption, however, can be approximately justified if the linear optical operations are fully characterized, which is the case in our scheme.

Finally, using the above purified encoding, we arrive at an equivalent entanglement-based scheme, where Alice makes random BB84 measurements on one half of a bipartite quantum state, and Bob makes random purified measurements on the other half. In this case, the security of ddiQKD follows directly from the one of BB84 QKD scheme, with the additional benefit in that the physics of the detectors is excluded from the security analysis. Particularly, the security can be obtained by using the entropic uncertainty relation proof technique [22, 28]. For instance, in the asymptotic limit, and under the approximations that the heralded single-photon source is a true single-photon source and the BB84 polarization states are prepared accurately, the secret key fraction is $\propto 1 - 2h(Q)$, where h is the binary entropy function and Q is the error rate of the sifted key. In fact, the finite-key security performance of ddiQKD is expected to be similar to the one of the single-photon BB84 [28] since only single-photon detections are required on Bob's side. Likewise, for a more practical implementation using decoy-state method for WCS, we expect the security performance to be similar to the one in Ref. [22].

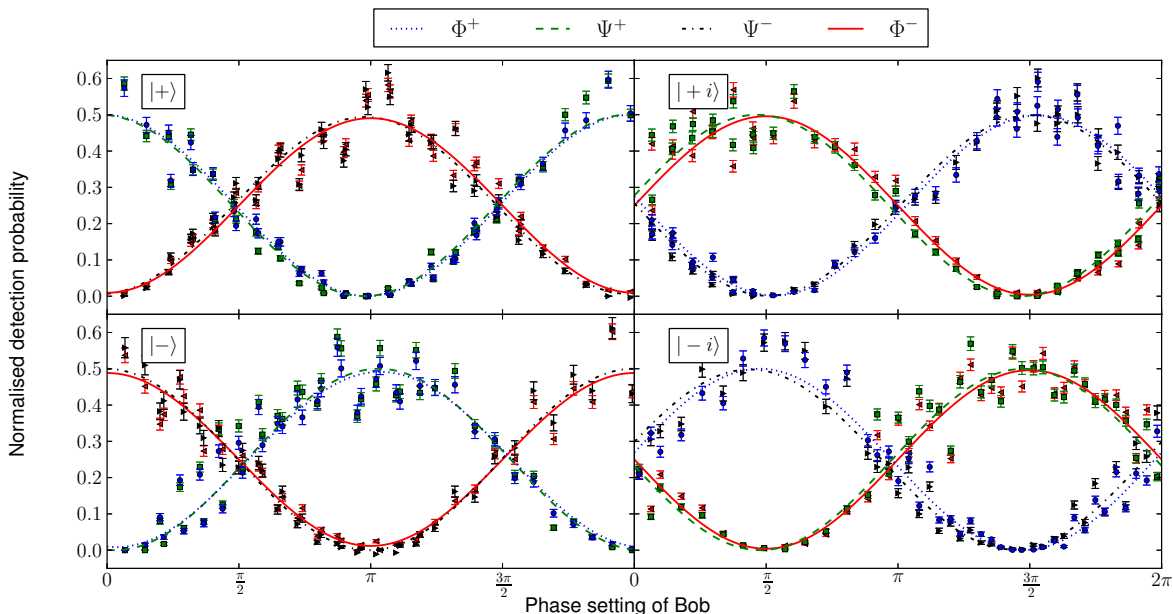


FIG. 3. Experimental Bell-state measurement outcomes as a function of the phase setting inside Bob's interferometer. Four sets of measurements are shown, one for each of the possible states sent by Alice.

IV. PROOF-OF-PRINCIPLE EXPERIMENT

We implemented a proof-of-principle experiment as illustrated in Fig. 2. The single-photon state preparation on Alice's side starts with the generation of a pair of correlated photons by type-0 SPDC in a fiber-pigtailed periodically poled lithium niobate waveguide (PPLN-WG). The waveguide is pumped with a diode laser (Toptica DL100) at 780 nm and the signal and idler photons are deterministically separated by dense wavelength division multiplexers at 1563.9 nm (200 GHz) and 1556.6 nm (100 GHz), respectively. The idler photon was detected by a free-running InGaAs single-photon detector (ID Quantique ID220). The polarization of the heralded signal photon was set to $|+\rangle$ before passing through a Soleil-Babinet, which allowed us to rotate the state around the equator of the Bloch sphere. Bob's trusted device consists of a balanced interferometer, with a polarization controller in the upper arm acting as a HWP and a piezo phase modulator in the lower arm. The outputs of the BSM corresponding to $|\Phi^-\rangle$ and $|\Psi^-\rangle$ were delayed by 2.5 ns before being combined using two PBSs (see Fig. 2) with the other two outputs, which allowed the use of just two detectors for all four outcomes. Bob's InGaAs single-photon detectors were cooled to -90°C using a Stirling cooler, which allowed them to exhibit a dark count rate of less than 50 cps in the free-running regime [29]. The detection events were recorded using a time-to-digital converting (TDC) module. The $g^{(2)}(0)$ of

the single-photons at Alice was about 10^{-3} in a 1 ns coincidence window. Due to the extremely low dark count probability of the InGaAs detectors used, the probability of having a double detection at Bob was $< 10^{-6}$.

To test the theoretical predictions and analyze the detection outcomes for all of the combinations of Alice and Bob's settings, we fixed the state prepared by Alice and scanned the phase of Bob's interferometer with a phase modulator. Figure 3 shows four curves, one for each of the polarization states chosen by Alice, representing the normalized probability of each Bell-state being announced at any given phase setting in Bob's interferometer. The measurement points were fitted with theoretical curves in order to calculate the visibility, with the highest average value obtained being $99.2 \pm 1.5\%$ for the $|-i\rangle$ input state at Bob and the lowest value of $96.0 \pm 2.1\%$ for the $|- \rangle$ state. In the real QKD protocol Bob would randomly select four phase settings corresponding to the BB84 states as outlined in section II. Table I shows the expected Bell-state announcement probability $\text{Pr}[k]$ for every combination of Alice and Bob's settings, where a white cell corresponds to $\text{Pr}[k] = 0$, light gray to $\text{Pr}[k] = 1/4$ and dark grey to $\text{Pr}[k] = 1/2$. We are able to complete this correlation table with the experimental results by selecting points from Fig. 3 closest to the desired settings at Bob. One can see that the experimental values coincide with the prediction very well and the overall quantum bit error rate $Q = 1.5 \pm 0.5\%$. The total coincidence rate was around 60 cps.

V. DISCUSSION

As mentioned previously, the ddiQKD scheme is not the same as mdiQKD since the detectors cannot be considered as a completely “black-box” possessed by the eavesdropper, Eve. Indeed, if Eve had access to the output ports of Bob’s PBSs she could carry out a trojan horse attack [30] in order to gain information about the phase setting of Bob’s interferometer. In practice this requirement is easily fulfilled since the detectors can be placed directly within Bob’s trusted location and he can control the information that goes out of his lab. However, the outcome of the BSM can be completely controlled by Eve be it through the input port of Bob or by any other means, meaning that the ddiQKD scheme is secure against all detector side-channel attacks.

In our proof-of-principle experiment we made use of a heralded single-photon source to fulfil the qubit assumption. One could simplify the implementation by using WCSs together with the decoy method to estimate the number of single-photon events. This would enable a fast ddiQKD implementation comparable to existing GHz clocked systems [31, 32].

We would like to highlight that the concept of TQSP entanglement employed in the ddiQKD scheme can be achieved by using any two DoFs of the single-photon,

hence our implementation is not a unique possibility. For example, Alice could begin by encoding a time-bin qubit followed by Bob adding a polarization qubit to the same photon.

VI. CONCLUSION

We have proposed and demonstrated experimentally a new QKD protocol, namely ddiQKD, which overcomes the main disadvantages of the mdiQKD protocol and offers the same level of security. Future work should focus on deriving a bound on the extractable key length in a finite key scenario. Due to significant similarities in the implementation requirements with existing high-clock rate QKD systems, it is expected that a high speed version of a ddiQKD demonstration is achievable in the near future, paving the way to practical detector-side-channel free systems.

VII. ACKNOWLEDGMENTS

We would like to acknowledge Nino Walenta for useful discussions and the Swiss NCCR QSIT project for financial support.

-
- [1] C. H. Bennett and G. Brassard, in *Proc. IEEE Int. Conf. on Comp., Sys. and Signal Process.* (Bangalore, 1984) pp. 175–179.
- [2] N. Gisin, G. Ribordy, W. Tittel, and H. Zbinden, *Reviews of Modern Physics* **74**, 145 (2002).
- [3] L. Lydersen, C. Wiechers, C. Wittmann, D. Elser, J. Skaar, and V. Makarov, *Nat. Photonics* **4**, 686 (2010).
- [4] H.-K. Lo, M. Curty, and B. Qi, *Physical Review Letters* **108**, 130503 (2012).
- [5] E. Biham, B. Huttner, and T. Mor, *Phys. Rev. A* **54**, 2651 (1996).
- [6] H. Inamori, *Algorithmica* **34**, 340 (2008).
- [7] S. L. Braunstein and S. Pirandola, *Physical Review Letters* **108**, 130502 (2012).
- [8] A. Rubenok, J. A. Slater, P. Chan, I. Lucio-Martinez, and W. Tittel, *Physical Review Letters* **111**, 130501 (2013).
- [9] Y. Liu, T.-Y. Chen, L.-J. Wang, H. Liang, G.-L. Shentu, J. Wang, K. Cui, H.-L. Yin, N.-L. Liu, L. Li, X. Ma, J. S. Pelc, M. M. Fejer, C.-Z. Peng, Q. Zhang, and J.-W. Pan, *Physical Review Letters* **111**, 130502 (2013).
- [10] T. Ferreira da Silva, D. Vitoreti, G. B. Xavier, G. C. do Amaral, G. P. Temporão, and J. P. von der Weid, *Physical Review A* **88**, 052303 (2013).
- [11] Z. Tang, Z. Liao, F. Xu, B. Qi, L. Qian, and H.-K. Lo, *Phys. Rev. Lett.* **112**, 190503 (2014).
- [12] W.-Y. Hwang, *Phys. Rev. Lett.* **91**, 57901 (2003).
- [13] H.-K. Lo, H.-F. Chau, and M. Ardehali, *Journal of Cryptology* **18**, 133 (2005), arXiv:0011056v3 [quant-ph].
- [14] X.-B. Wang, *Phys. Rev. Lett.* **94**, 230503 (2005).
- [15] L. Vaidman and N. Yoran, *Phys. Rev. A* **59**, 116 (1999).
- [16] N. Lütkenhaus, J. Calsamiglia, and K.-A. Suominen, *Phys. Rev. A* **59**, 3295 (1999).
- [17] R. Valivarthi, I. Lucio-Martinez, A. Rubenok, P. Chan, F. Marsili, V. B. Verma, M. D. Shaw, J. A. Stern, J. A. Slater, D. Oblak, S. W. Nam, and W. Tittel, *Opt. Express* **22**, 24497 (2014).
- [18] Y.-L. Tang, H.-L. Yin, S.-J. Chen, Y. Liu, W.-J. Zhang, X. Jiang, L. Zhang, J. Wang, L.-X. You, J.-Y. Guan, D.-X. Yang, Z. Wang, H. Liang, Z. Zhang, N. Zhou, X. Ma, T.-Y. Chen, Q. Zhang, and J.-W. Pan, (2014), arXiv:1407.8012.
- [19] The security parameter of a QKD system is defined as the overall probability for the protocol to fail, leaking at least 1 bit of information to the adversary.
- [20] B. Korzh, C. C. W. Lim, R. Houlmann, N. Gisin, M. J. Li, D. Nolan, B. Sanguinetti, R. Thew, and H. Zbinden, (2014), arXiv:1407.7427.
- [21] M. Curty, F. Xu, W. Cui, C. C. W. Lim, K. Tamaki, and H.-K. Lo, *Nature communications* **5** (2014), 10.1038/ncomms4732.
- [22] C. C. W. Lim, M. Curty, N. Walenta, F. Xu, and H. Zbinden, *Physical Review A* **89**, 022307 (2014).
- [23] D. Boschi, S. Branca, F. De Martini, L. Hardy, and S. Popescu, *Phys. Rev. Lett.* **80**, 1121 (1998).
- [24] Q. Liu, A. Lamas-Linares, C. Kurtsiefer, J. Skaar, V. Makarov, and I. Gerhardt, *Review of Scientific Instruments* **85** (2014), arXiv:1307.5951.
- [25] V. Scarani, A. Acín, G. Ribordy, and N. Gisin, *Physical Review Letters* **92**, 057901 (2004).
- [26] D. Gottesman, H.-K. Lo, N. Lutkenhaus, and J. Preskill, *Quant. Inf. Comput.* **5**, 325 (2004).

- [27] N. J. Beaudry, M. Lucamarini, S. Mancini, and R. Renner, *Phys. Rev. A* **88**, 62302 (2013).
- [28] M. Tomamichel, C. C. W. Lim, N. Gisin, and R. Renner, *Nat Commun* **3**, 634 (2012).
- [29] B. Korzh, N. Walenta, T. Lunghi, N. Gisin, and H. Zbinden, *Applied Physics Letters* **104**, 081108 (2014).
- [30] N. Gisin, S. Fasel, B. Kraus, H. Zbinden, and G. Ribordy, *Physical Review A* **73**, 22320 (2006).
- [31] N. Walenta, a. Burg, D. Caselunghe, J. Constantin, N. Gisin, O. Guinnard, R. Houlmann, P. Junod, B. Korzh, N. Kulesza, M. Legré, C. W. Lim, T. Lunghi, L. Monat, C. Portmann, M. Soucarros, R. T. Thew, P. Trinkler, G. Trollet, F. Vannel, and H. Zbinden, *New Journal of Physics* **16**, 013047 (2014), 1309.2583.
- [32] M. Lucamarini, K. A. Patel, J. F. Dynes, B. Fröhlich, A. W. Sharpe, A. R. Dixon, Z. L. Yuan, R. V. Penty, and A. J. Shields, *Opt. Express* **21**, 24550 (2013).